OCEAN CIRCULATION

Strengthening of the Kuroshio current by intensifying tropical cyclones

Yu Zhang[1]*, Zhengguang Zhang[1], Dake Chen[2,3], Bo Qiu[4], Wei Wang[1]

A positive feedback mechanism between tropical cyclones (TCs) and climate warming can be seen by examining TC-induced energy and potential vorticity (PV) changes of oceanic geostrophic eddies. We found that substantial dissipation of eddies, with a strong bias toward dissipation of anticyclonic eddies, is directly linked to TC activity. East of Taiwan, where TCs show a remarkable intensifying trend in recent decades, the ocean exhibits a corresponding upward trend of positive PV anomalies. Carried westward by eddies, increasing numbers of positive PV anomalies impinge on the Kuroshio current, causing the mean current to accelerate downstream. This acts in opposition to decreasing basin-scale wind stress and has a potentially important warming impact on the extratropical ocean and climate.

In a warming climate, very intense tropical cyclones (TCs; categories 4 and 5 on the Saffir-Simpson scale) are becoming more intense and frequent, as proposed by theoretical and modeling studies (*1*–*4*) and supported by observations (*5*, *6*). This behavior raises the question of what feedbacks can be induced by TC changes on climate. Much prior work has been focused on TCs' interaction with the quiescent upper ocean. For example, the decay of cold ocean wakes produced by storm-driven mixing causes net heating of the upper ocean and has been suggested to have important effects on global climate (*7*, *8*). The ocean is anything but quiescent or uniform, though, and is full of dynamical structures of different scales. Among them, rotating structures with spatial scales of order O (10 to 100 km), temporal scales of order O (100 days), and vertical extents of 1000 m or more, usually referred to as mesoscale eddies, are the most ubiquitous and energetic; they play an essential role in transporting material and energy, and they modulate large-scale ocean circulation (*9*–*11*).

Because mesoscale eddies are ubiquitous, their encounters with TCs are not rare. By modulating subsurface density as well as thermal conditions, these synoptic-scale structures have been found to greatly affect the evolution of a storm's strength, posing a big challenge for operational prediction of TC intensity (*12*–*15*). Meanwhile, TCs can also have a large impact on eddies through more than one mechanism and in different or opposite ways. For example, in central areas of TCs, strong and positive wind stress curl dominates, producing divergent surface currents, forcing cool water upward from below, and elevating isopycnals as much as 100 m, in the same sense as the circulation of cyclonic eddies and the associated upward displacements of isopycnals. Hence, oceanic cyclonic eddies can be enhanced or generated (*16*–*18*) while their mirror images, anticyclonic eddies, can be weakened. In outer regions of TCs, the wind stress curl is negative and very weak. Although the effects are to strengthen anticyclonic eddies yet weaken cyclonic eddies, opposite to those inside TCs' cores, the amplitudes are much reduced. In the meantime, at the smallest scale satisfying geostrophy, mesoscale eddies are always close to geostrophic balance. If this balance is disturbed through processes such as the shoaling of isopycnals by strong storms, the flow will adjust itself back to a state of geostrophic balance. This process, known as geostrophic adjustment, was first considered by Rossby in 1938 (*19*) and has since been investigated in a variety of contexts both linear and nonlinear (*20*–*23*). Common to all those studies is that the flows in question hold less energy at their end states than they do initially, and energy is dispersed in the form of inertial gravity waves (*19*, *24*). It is therefore anticipated that eddies under the influence of strong storms may be perturbed and subsequently undertake adjustment processes that attenuate them (*25*).

Evidence continues to mount that both mechanisms described above exist, working together to reduce the strength of anticyclonic eddies but acting against each other in changing cyclonic eddies. Which process dominates, and what overall influence the TCs exert on an underlying eddy field, remains unclear. To this end, a survey of eddies' lifetime evolution—in particular, immediately after their meeting with TCs—is necessary. The advent of satellite altimetry has enabled global and synoptic mapping of eddies with prominent surface signatures (*26*). The later combination of data from two altimeters has provided a time-series record of global maps of ocean eddies at high spatial and temporal resolutions [DT-2014 daily "two-sat merged" gridded product provided by archiving, validation, and interpretation of satellite oceanographic data (AVISO) (*27*)]. On the basis of that record, an eddy-tracking data archive was constructed, providing at daily frequency the center, amplitude, polarity, radius, and rotational velocity for those eddies identified and tracked by altimetry (*28*). In addition, Argo floats have provided depth profiles of temperature and salinity, from which eddies' vertical structures can be extracted (*29*). Taking advantage of both AVISO and Argo data, a law for the universal structure of

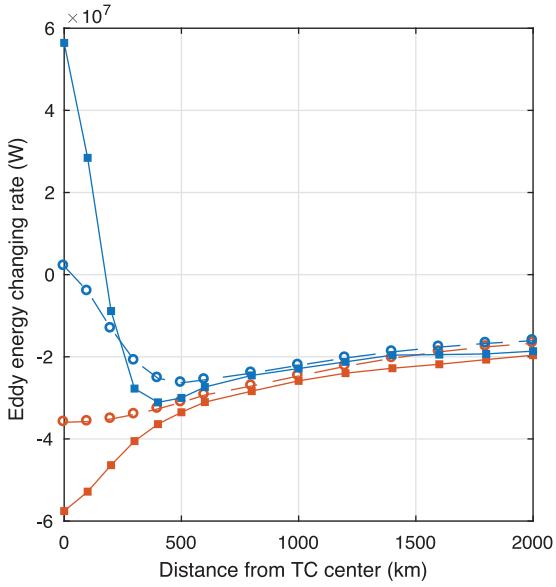

Fig. 1. Changing rate of eddy energy versus distance from TC center. Mean changing rate of eddies' total energy is plotted against radial distance, averaged over 15 days after passing of TCs, for anticyclonic eddies (red curves) and cyclonic eddies (blue curves). Curves with circles are for all TCs in the western North Pacific Ocean between 1993 and 2014; those with squares are for more intense winds with speed greater than 40 m s^{-1}.

[1]Physical Oceanography Laboratory/CIMST, Ocean University of China and Qingdao National Laboratory for Marine Science and Technology, Qingdao, P. R. China. [2]State Key Laboratory of Satellite Ocean Environment Dynamics, Second Institute of Oceanography, Ministry of Natural Resources, Hangzhou, P. R. China. [3]Southern Marine Science and Engineering Guangdong Laboratory (Zhuhai), Zhuhai, P. R. China. [4]Department of Oceanography, University of Hawai'i at Manoa, Honolulu, HI, USA.
*Corresponding author. Email: yuz@ouc.edu.cn

eddies was uncovered (*30*), making it possible to accurately infer an eddy's three-dimensional structure from its surface signal. Using 20 years of these datasets in combination with TC observations in the western North Pacific, we carried out an analysis of the evolution of three-dimensional eddy energy and potential vorticity fields with a special focus on storm effects. [Potential vorticity (PV) is a dynamically conserved quantity depicting the tendency of a rotating fluid to spin.] Our results indicate that the interaction with TCs can introduce an important, newly recognized feature of the eddy field, which, together with the strengthening trend of TCs in a warming climate, has potentially strong influence on large-scale ocean circulation and climate.

Eddy response to TCs

Figure 1 shows the results of a survey of the rates of energy change of eddies during the 15-day period after their encounters with TCs in the western North Pacific Ocean (see supplementary materials). The rate of change depends on factors including storm wind speed, eddy polarity, and the radial distance, *r*, between an eddy and the storm's center at the time of meeting.

Cyclonic and anticyclonic eddies show obvious differences with little asymmetry about the storm track (see supplementary materials), especially under strong winds. Anticyclonic eddies that have passed within ~1000 km of the storm center generally experience substantial weakening afterward. On average, the energy decay rate declines from the storm center monotonically outward, asymptotically approaching the background dissipation level that is weaker than the central maximum value by a factor of 2 to 3 (red curves in Fig. 1). Cyclonic eddies' responses, although close to those of anticyclonic eddies' responses farther away from the storm, exhibit a tendency to strengthen progressively as they approach the storms' centers (blue curves in Fig. 1). Thus, TCs not only cause the entire eddy field to decay substantially more quickly than otherwise might have occurred but also make cyclonic eddies relatively stronger than anticyclonic eddies.

As seasonal phenomena, TCs develop mostly during the months of June through November, with peak activity occurring usually in late summer (*31*). If TCs' effect is dominant in driving eddy dissipation, the year-round energy evolution of eddies should exhibit similar seasonality.

In the North Pacific Ocean, only two areas demonstrate strong seasonal variation of the decay rates of eddies (Fig. 2A), and both are near the western boundary: One located at 20° to 30°N and 120° to 130°E, east of Taiwan, coincides with the region of the strongest TC activity (solid contours in Fig. 2A); the other one is located in the Kuroshio Extension. Both regions are prominent for vigorous eddy fields, but they differ from each other in two important aspects. First, their energetic eddy fields have different origins. In the Kuroshio Extension region, a high eddy kinetic energy level arises from the meandering of the current itself (*32*), while along latitudes around 25°N, eddies are generated in the shearing flows between the eastward Subtropical Counter Current located in the 18° to 25°N band and the underlying westward North Equatorial Current (*33*). After generation, these eddies propagate mainly westward at speeds of a few centimeters per second, evolve as they move, enter and pass through the region of strong TC activity, and finally collide with the Kuroshio before they disappear (*32*). Second, seasonal variations of the eddies' decay rates in the two regions have different origins. In the TC-active region, the seasonal variation of the decay rate is in phase with that of TC activity (Fig. 2B), and so is the difference of decay rates between anticyclonic and cyclonic eddies (see supplementary materials). Both pieces of evidence indicate TCs' vital role in causing eddy dissipation. In the Kuroshio Extension region, the seasonal variation of the decay rate is almost 180° out of phase with that in the south, being strong in winter and spring but weak in summer and autumn (Fig. 2C). A closer look at different factors contributing to eddies' energy evolution reveals that the seasonality of the decay rate in this area is primarily due to the seasonally varying ocean stratification. Following the seasonal variation of solar irradiance, the buoyancy flux across the air-sea interface changes, as does

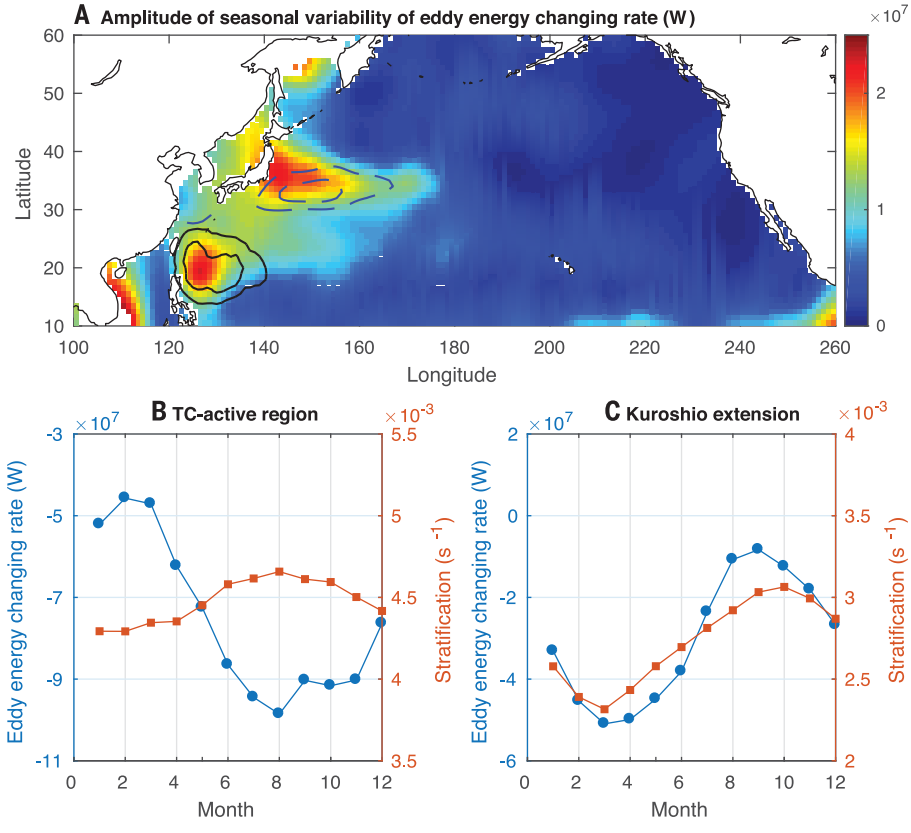

Fig. 2. Seasonal variation of eddy energy changing rate. (**A**) Seasonal variation amplitude of eddy energy changing rate in the North Pacific Ocean (color scale). TC intensity, defined as annual accumulated power input of TCs to the ocean, $\sum v^3$ (where v is the local instantaneous wind speed from the Best Track Dataset of Tropical Cyclones), is shown as solid contours. Seasonal variation amplitudes of oceanic stratification are shown as dashed contours. See supplementary materials for details. (**B** and **C**) Seasonal variation of eddy energy changing rate (blue) as compared with seasonal variation of oceanic stratification (red) in the TC-active region (120° to 130°E, 20° to 30°N) (B) and the Kuroshio Extension region (C). A 3-month running mean smoothing was applied to the time series.

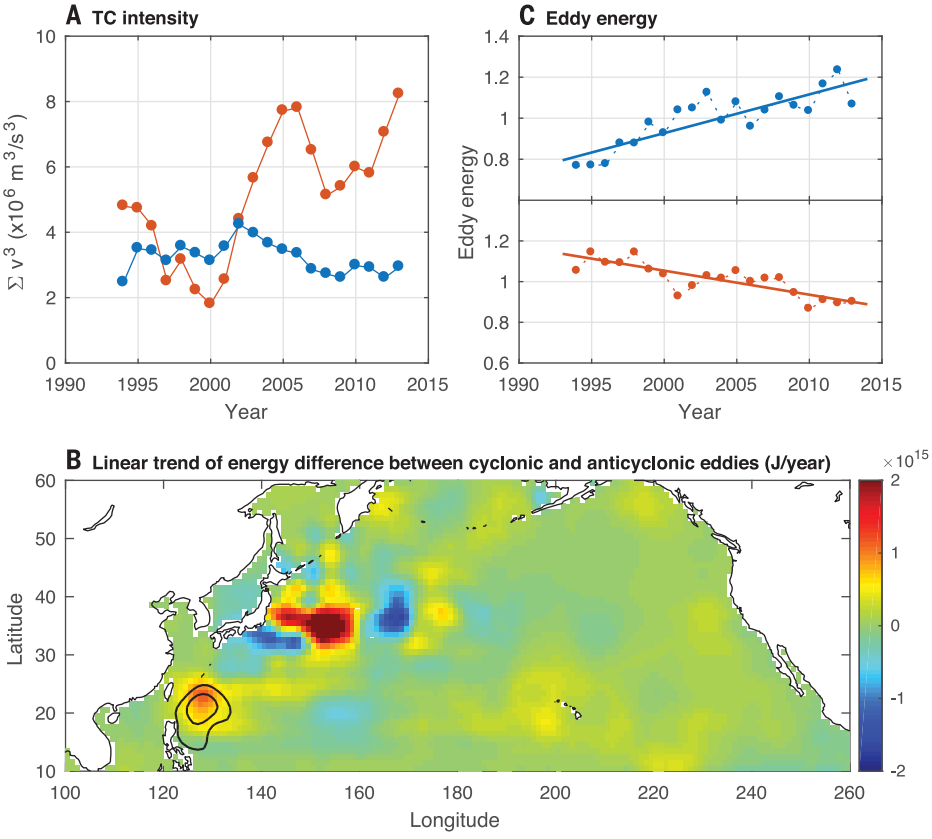

Fig. 3. Time series of TC intensity and energy difference between cyclonic eddies and anticyclonic eddies. (**A**) Time series of TC intensity, defined as annual accumulated power input in the TC-active area with winds below 40 m s^{-1} (blue) and above 40 m s^{-1} (red), from 1993 to 2014. (**B**) Linear trend of energy difference between cyclonic eddies and anticyclonic eddies in the North Pacific Ocean (color scale). Linear trend of TCs' annual accumulated power input is shown by contours. (**C**) Time series of normalized volume-integrated energy of cyclonic eddies (upper, blue dots) and anticyclonic eddies (lower, red dots) in the TC-active area. Linear trends are shown by solid lines. A 3-year running mean smoothing was applied to the time series. Each time series was normalized by dividing by its own 20-year mean.

the stratification in the ocean interior, which, as one of the most essential environmental factors shaping eddy characteristics, further modulates their energy and the associated evolution process. Near the tropics, both solar heating and ocean stratification change less across different seasons than they do at higher latitudes (dashed contours in Fig. 2A), whereas TC activity is much stronger, leaving TCs' seasonal forcing largely responsible for the seasonality of eddies' decay.

Our eddy energy analysis is performed in a Lagrangian framework (see supplementary materials): For each eddy identified by altimetry, the sum of kinetic and available potential energy is calculated on a daily basis along its track, and the 15-day low-pass–filtered changing rate is subsequently computed. More important, the volume integration instead of the surface component of energy is evaluated so as to include the effect of ocean stratification in driving the seasonality of the energy decay.

The TC-active region east of Taiwan (20° to 30°N, 120° to 130°E) not only has the strongest storms on average but also has displayed an obvious trend in TC intensity over the past decades, primarily due to intensified very strong storms (winds with speed above 40 m s^{-1}; Fig. 3A). Because intense TCs are inclined to induce greater dissipation of anticyclonic eddies but to cause moderate to weak dissipation, or even discernible strengthening, of cyclonic eddies, we anticipate relatively more energetic cyclonic eddies than anticyclonic eddies under intensifying TC activity. This expectation is confirmed by a trend analysis of energy difference between cyclonic and anticyclonic eddies in the entire basin. The result yields two regions of peak signals (Fig. 3B); the southern one located around 25°N displays a strong positive trend resulting from the strengthening of cyclonic eddies and the concurrent weakening of anticyclonic eddies (Fig. 3C). The region is nearly contiguous with the TC-active area (solid contours in Fig. 3B). Furthermore, its remarkable amplitude makes it distinct and isolated from both the neighboring areas and the latitudinal band farther to the east, from where eddies seen in this region are propagating. Therefore, the difference between the two types of eddies in this region is unlikely to be the result of any remote forcing. Instead, the strengthening of local TC activity introduces this new feature of the eddy field.

The Kuroshio Extension shows distinctly different trends between cyclonic eddies and anticyclonic eddies but with signs alternating zonally along the flow axis (Fig. 3B). Because eddies here are formed mostly by the pinch-off process of meanders, eddies generated from northward meanders are anticyclonic eddies with anomalous warm water at the core, and those generated from southward meanders are cyclonic eddies with cold cores. In other words, north of the flow axis, anticyclonic eddies tend to dominate, whereas to the south cyclonic eddies prevail; however, with the meridional migration of the flow axis, the relative strength of the two types of eddies will be changed. For example, a region previously dominated by anticyclonic eddies will be filled with more cyclonic eddies as the axis moves to the north. Presumably the strong signals with alternating signs are related to spatial migration of the current axis, which is inhomogeneous in the zonal direction (*34*); these signals result from the redistribution of eddies but do not reflect net changes of the eddy field as a whole. Therefore, the only robust strengthening trend of cyclonic eddies relative to anticyclonic eddies in the North Pacific Ocean is the TC-driven trend east of Taiwan.

Strengthening of the Kuroshio current by eddies

The Kuroshio is primarily wind-driven. As the western boundary current of the North Pacific subtropical gyre, it acts as the return limb for the southward interior Sverdrup flow that is controlled by the basin-scale wind stress curl (*32*). Nonetheless, many other factors besides the basin-scale wind, such as the El Niño–Southern Oscillation (ENSO), the Pacific Decadal Oscillation (PDO), and the local wind stress and topography, influence it as well (*35*–*37*). In particular, eddy activity has

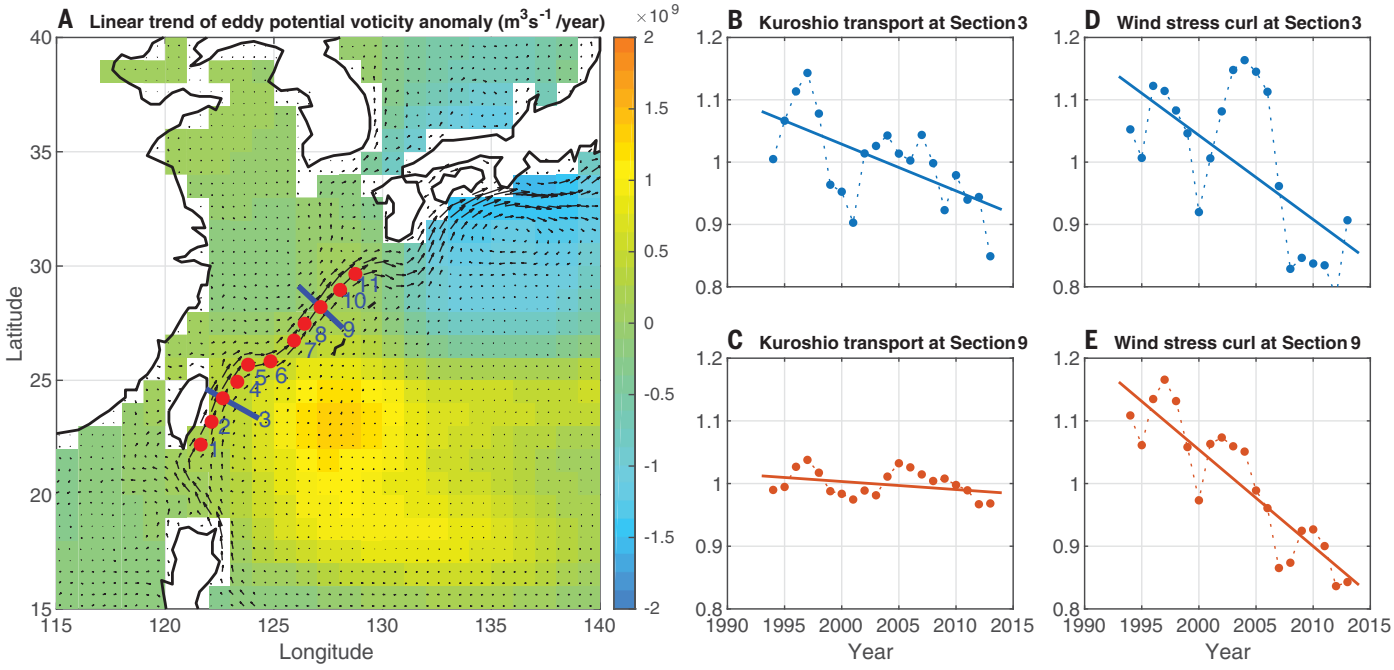

Fig. 4. Variation of Kuroshio transport along its path. (**A**) Linear trend of eddy potential vorticity (PV) anomaly in the western North Pacific Ocean (color scale). Mean velocity (arrow directions and lengths indicate direction and magnitude of velocity), coastlines (contour), and locations of cross sections (red dots) are shown. Sections 3 and 9 are denoted by solid blue lines. (**B**) Time series of normalized Kuroshio transport across section 3 (blue). (**C**) Same as (B) but for section 9 (red). (**D**) Time series of normalized strength of the wind stress curl (blue) zonally averaged across the basin and meridionally within the latitudinal range of section 3 (20° to 25°N). (**E**) Same as (D) but for section 9 (25° to 30°N). Dots denote annual mean values with a 3-year running mean smoothing applied; solid lines denote linear trends. The Kuroshio transport across each section was calculated as the along-section integration of perpendicular surface geostrophic velocity. In (B) to (E), each time series was normalized by dividing by its own 20-year mean.

been suggested as a main modulator of the Kuroshio east of Taiwan (*37*, *38*). Because this segment of the Kuroshio is also on the western edge of the TC-active region, a question naturally arises as to how the current is affected by the strengthening trend of cyclonic eddies relative to anticyclonic eddies discussed above.

The eddy flux of potential vorticity (PV) is the key to answering this question, because it comprehensively reflects the dynamical and thermodynamical links between the mean and eddy components of the flow field (*39*). A crucial difference between a cyclonic and an anticyclonic eddy is that the former has a positive PV anomaly while the latter has a negative one, both of which are carried westward like passive tracers by these fairly nonlinear and isolated eddies. Because cyclonic eddies are relatively stronger than anticyclonic eddies, the associated positive PV anomaly prevails (Fig. 4A), leading to a westward flux of net positive PV anomaly toward the mean current. According to the turbulent Sverdrup balance theorized by Rhines and Holland in 1979 (*40*), the westward positive eddy PV flux works to increase the PV of the mean component by accelerating the current northward (see supplementary materials). As shown below, this is the underlying mechanism for the downstream acceleration of the Kuroshio in recent decades.

In the past two decades (1994–2013), Kuroshio transport east and downstream of Taiwan has undergone an obvious decreasing trend. The trend has been ascribed to the weakening of the subtropical wind stress curl (*41*), which, according to the classical Sverdrup balance, sets the transport of the western boundary current (*42*), but apparently this is not the whole story. For example, across both section 3 and section 9, the Kuroshio transport was noticeably weakened, but the upstream transport was reduced more remarkably: a 13% decrease at section 3 (Fig. 4B) versus a 3% decline at section 9 (Fig. 4C). Meanwhile, the strength of the basin-scale wind stress curl within this latitudinal band experienced a much greater decline than that of the Kuroshio transport, and the reduction amplitude slightly strengthened northward: a 27% decrease around the latitudes of section 3 (Fig. 4D) versus a more vigorous one, 31%, at section 9 (Fig. 4E). Therefore, some other factors must be accelerating the Kuroshio and counteracting the decelerating effects of the basin-scale wind.

To get a clearer picture, we take the difference between the two sections. The difference of Kuroshio transport reveals a large positive trend suggesting that the flow has increased downstream in the past 20 years (Fig. 5A). The difference of the strength of the basin-scale wind stress curl, however, demonstrates a slight downward trend, corresponding to a tendency for downstream deceleration of the current (Fig. 5B). Hence, the classical Sverdrup balance depicting the dominant role of the basin-scale wind field cannot explain the observed acceleration of the current, and therefore, consistent with the turbulent Sverdrup balance theory, eddy PV flux is implicated.

Calculation of the eddy PV flux (see supplementary materials) between the two sections yields a curve (Fig. 5C) that is in good agreement with the downstream transport change (correlation coefficient of 0.69) in terms of both the interannual variability and the long-term upward trend. Moreover, at other locations along the current axis from south of Taiwan toward south of Japan (red dots in Fig. 4A), trends of the downstream change of Kuroshio transport and trends of the corresponding eddy PV flux (Fig. 5D) show a linear relation between the two that is consistent with our theoretical prediction.

All the above pieces of evidence point to the eddy effect as the reason for the increasing strength of Kuroshio transport despite the weakening basin-scale wind stress curl, indicating a linkage between TC activity and

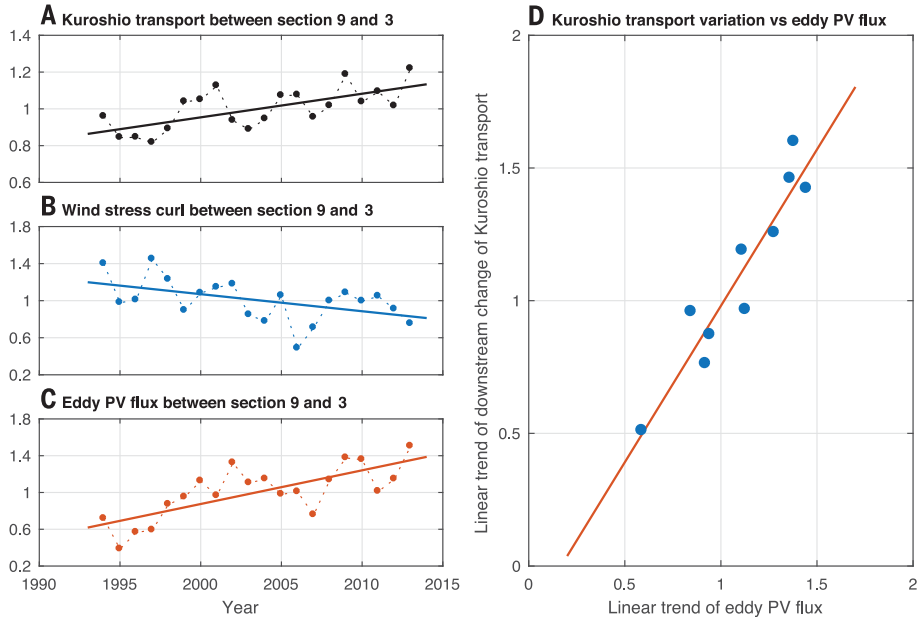

Fig. 5. Modulation of Kuroshio transport by eddy potential vorticity (PV) flux. (**A**) Time series of normalized Kuroshio transport difference between section 9 and section 3 (black). (**B**) Same as (A) but for the normalized strength of the wind stress curl zonally averaged across the basin (blue). (**C**) Same as (A) but for the normalized eddy PV flux (see supplementary materials) in the area bounded by the two sections (red). Dots denote annual mean with a 3-year running mean smoothing applied; solid lines denote linear trends. (**D**) Scatterplot of linear trends of the normalized Kuroshio transport difference between section 2, 3, 4, 5, 6, 7, ..., 11 and section 1, and linear trends of the normalized eddy PV flux in corresponding areas. Linear fitting result is shown as a solid line. In (A) to (C), each time series was normalized by dividing by its own 20-year mean.

the Kuroshio transport change. Relative to TCs, oceanic eddies usually have much longer life spans and much slower translation speeds. Thus, eddies facilitate slow oceanic responses to TCs' more rapid forcing, which would further feed back onto the longer-term variations of the large-scale ocean circulation and climate change through eddy–mean flow interactions.

Conclusions

The kinetic energy of the ocean circulation is dominated by mesoscale eddies, which have been receiving much attention since they were first discovered in the early 1960s. Here, we have demonstrated a linkage between TC forcing and the substantial decay of the underlying eddy field, from which energy is transferred progressively downscale to smaller scales that are vulnerable to dissipation and mixing processes. Moreover, this decay process has pronounced seasonality due to the seasonal variation of TC occurrence, which paces the downscale energy cascade as well as the enhancement of the related mixing in the deep ocean. Finally, we have shown that the modification of the eddy field by TCs results in a positive feedback between TCs and climate change by modifying Kuroshio transport.

As the western boundary current of the North Pacific Ocean, the Kuroshio serves as a conduit for transporting warm water northward from its equatorial source region, thus playing a crucial role in modulating the ocean and climate in mid- to high latitudes (*43*, *44*). As a result of global warming in recent decades, the western Pacific Warm Pool has warmed notably, which may cause more heat to be carried northward by the Kuroshio, although to some extent this could be moderated by the weakening of Kuroshio transport. Global warming also may cause more intense TCs to occur at a higher frequency, which should increase the ratio of cyclonic eddies to anticyclonic eddies and thereby increase the trend of positive eddy-PV flux impinging onto the Kuroshio. That should accelerate downstream transport and contribute to further warming at higher latitudes. Notwithstanding the lack of a quantitative determination of the warming effect of TCs, it seems quite likely that overlooking this positive feedback mechanism could induce measurable bias in climate predictions. For a proper representation of eddies in climate models, more theoretical and modeling studies are needed to improve our understanding of the physical processes involved in the interactions among eddies, TCs, and large-scale ocean circulation.

REFERENCES AND NOTES

1. K. A. Emanuel, *Nature* **326**, 483–485 (1987).
2. G. J. Holland, *J. Atmos. Sci.* **54**, 2519–2541 (1997).
3. K. Oouchi *et al.*, *J. Meteorol. Soc. Jpn.* **84**, 259–276 (2006).
4. K. A. Emanuel, *Proc. Natl. Acad. Sci. U.S.A.* **110**, 12219–12224 (2013).
5. K. Emanuel, *Proc. Natl. Acad. Sci. U.S.A.* **114**, 12681–12684 (2017).
6. Y. K. Lim, S. D. Schubert, R. Kovach, A. M. Molod, S. Pawson, *Sci. Rep.* **8**, 16172 (2018).
7. K. Emanuel, *J. Geophys. Res.* **106**, 14771–14781 (2001).
8. M. F. Jansen, R. Ferrari, *Geophys. Res. Lett.* **36**, L06604 (2009).
9. R. Ferrari, C. Wunsch, *Tellus A* **62**, 92–108 (2010).
10. R. Ferrari, C. Wunsch, *Annu. Rev. Fluid Mech.* **41**, 253–282 (2009).
11. Z. Zhang, W. Wang, B. Qiu, *Science* **345**, 322–324 (2014).
12. B. Jaimes, L. K. Shay, *Mon. Weather Rev.* **136**, 4188–4207 (2009).
13. L. K. Shay, G. J. Goni, P. G. Black, *Mon. Weather Rev.* **128**, 1366–1383 (2000).
14. N. D. Walker *et al.*, *Geophys. Res. Lett.* **41**, 7595–7601 (2014).
15. C.-C. Wu, C.-Y. Lee, I.-I. Lin, *J. Atmos. Sci.* **64**, 3562–3578 (2007).
16. L. Sun *et al.*, *J. Geophys. Res. Oceans* **119**, 5585–5598 (2014).
17. X. Shang, H. Zhu, G. Gen, C. Xu, Q. Yang, *Adv. Meteorol.* 340432 (2015).
18. Z. Lu, G. Wang, X. Shang, *J. Phys. Oceanogr.* **46**, 2403–2410 (2016).
19. C.-G. Rossby, *J. Mar. Res.* **1**, 239–263 (1938).
20. A. E. Gill, *J. Fluid Mech.* **77**, 603–621 (1976).
21. H. W. Ou, *J. Phys. Oceanogr.* **14**, 994–1000 (1984).
22. A. C. Kuo, L. M. Polvani, *J. Fluid Mech.* **394**, 1–27 (1999).
23. A. Coutino, M. Stastna, *Nonlin. Processes Geophys.* **24**, 61–75 (2017).
24. A. Cahn Jr., *J. Meteorol.* **2**, 113–119 (1945).
25. B. Jaimes, L. K. Shay, *J. Phys. Oceanogr.* **40**, 1320–1337 (2010).
26. L.-L. Fu, *J. Geophys. Res.* **88**, 4331–4341 (1983).
27. N. Ducet, P. Y. Le Traon, G. Reverdin, *J. Geophys. Res.* **105**, 19477–19498 (2000).
28. D. B. Chelton, M. G. Schlax, R. M. Samelson, *Prog. Oceanogr.* **91**, 167–216 (2011).
29. J. Gould *et al.*, *Eos* **85**, 179–184 (2004).
30. Z. Zhang, Y. Zhang, W. Wang, R. X. Huang, *Geophys. Res. Lett.* **40**, 3677–3681 (2013).

31. K. Emanuel, *Annu. Rev. Earth Planet. Sci.* **31**, 75–104 (2003).
32. B. Qiu, in *Encyclopedia of Ocean Sciences* (Academic Press, 2001), pp. 1413–1426.
33. B. Qiu, *J. Phys. Oceanogr.* **29**, 2471–2486 (1999).
34. B. Qiu, S. Chen, N. Schneider, *J. Clim.* **30**, 9591–9605 (2017).
35. C. Hwang, R. Kao, *Geophys. J. Int.* **151**, 835–847 (2002).
36. C.-R. Wu, *Prog. Oceanogr.* **110**, 49–58 (2013).
37. D. Zhang, T. N. Lee, W. E. Johns, C.-T. Liu, R. Zantopp, *J. Phys. Oceanogr.* **31**, 1054–1074 (2001).
38. Y.-C. Hsin, *J. Geophys. Res. Oceans* **120**, 1792–1808 (2015).
39. G. K. Vallis, *Atmospheric and Oceanic Fluid Dynamics* (Cambridge Univ. Press, 2006).
40. P. B. Rhines, W. R. Holland, *Dyn. Atmos. Oceans* **3**, 289–325 (1979).
41. Y.-L. Wang, C.-R. Wu, *Sci. Rep.* **8**, 14633 (2018).
42. J. Pedlosky, *Geophysical Fluid Dynamics* (Springer, ed. 2, 1987).
43. H. Bryden, S. Imawaki, in *Ocean Circulation and Climate*, G. Siedler, J. Church, J. Gould, Eds. (Academic Press, 2001), pp. 455–474.
44. Y.-O. Kwon *et al.*, *J. Clim.* **23**, 3249–3281 (2010).

ACKNOWLEDGMENTS

We acknowledge discussions with J. Pedlosky. **Funding:** Supported by National Natural Science Foundation grants 41722602, 41730535, and 41876007; National Basic Research Priorities Program of China grant 2015CB954300; and National Program on Global Change and Air-Sea Interaction grant GASI-IPOVAI-04.
Author contributions: Y.Z. and W.W. conceived the project and developed data analysis methodology; Y.Z., Z.Z., and W.W. carried out data analyses; Y.Z. wrote the manuscript; and B.Q. and D.C. reviewed and edited the manuscript. **Competing interests:** The authors declare that they have no competing interests. **Data and materials availability:** The sources of the data used in this paper are listed in the supplementary materials.

SUPPLEMENTARY MATERIALS

science.sciencemag.org/content/368/6494/988/suppl/DC1
Materials and Methods
Figs. S1 and S2
References (*45*–*47*)

7 April 2019; accepted 30 March 2020
10.1126/science.aax5758

Science

Strengthening of the Kuroshio current by intensifying tropical cyclones

Yu Zhang, Zhengguang Zhang, Dake Chen, Bo Qiu and Wei Wang

Science **368** (6494), 988-993.
DOI: 10.1126/science.aax5758

Changing forces in midstream

The intensity and frequency of the strongest cyclones east of Taiwan have increased over the past several decades as the climate has warmed. Zhang *et al.* found that one result of this trend has been the strengthening of Kuroshio current transport off the coast of Japan. The Kuroshio, like its Atlantic counterpart the Gulf Stream, is a surface current that moves huge volumes of warm water from low latitudes to high ones. As strong Pacific cyclones have become stronger, they have increased the amount of energy contained in cyclonic mesoscale ocean eddies and decreased that of anticyclonic ones. This in turn has increased the transfer of energy to the Kuroshio as eddies move into the current, providing a feedback between climate warming and ocean heat transport.

Science, this issue p. 988